Mechanical Properties of a Heat-Treatable Al-Sc Alloy Reinforced with Al_2O_3 Dispersoids

Richard A. Karnesky[1], Liang Meng[1,2], David N. Seidman[1], David C. Dunand[1]

[1]Northwestern University, Department of Materials Science & Engineering, 2220 Campus Dr., Evanston, IL 60208, USA.
[2]Zhejiang University, Department of Materials Science and Chemical Engineering, Hangzhou 310027, PRC.

Keywords: Aluminum alloys, Scandium, Alumina, Mechanical properties, Precipitation strengthening, Dispersoid strengthening, Creep, Threshold stress

Abstract

The mechanical behavior of precipitation-strengthened Al-0.18 wt.% Sc alloys containing 30 vol.% Al_2O_3 dispersoids is studied at 25, 300 and 350°C. The effect of Al_3Sc precipitate size is studied by varying aging treatments. Microhardness measurements show that both populations of particles (nanometer-sized Al_3Sc precipitates and submicron-sized Al_2O_3 dispersoids) contribute to strength at ambient temperature. At elevated temperature, a threshold stress is observed, indicative of interactions between matrix dislocations and the particles. The threshold stress is significantly higher than either Al-0.18 wt.% Sc alloys without Al_2O_3 dispersoids or Al-30 vol.% Al_2O_3 without Al_3Sc precipitates. This indicates that strengthening is occurring at both length scales and in a nonlinear manner, as the reinforced alloy exhibits strength higher than the sum of the strengths of Al-Sc and Al-Al_2O_3 alloys.

Introduction

During the past three decades [1], aluminum alloy matrix composites reinforced with ceramic particles have held significant potential for engineering applications due to their high strength, high stiffness, and improved wear and corrosion resistance [2]. They can be used at elevated temperatures because of the stability of the reinforcements. Creep resistance properties are important for many high temperature applications. In addition to the parameters of the reinforcing phase (composition, shape, volume fraction, distribution homogeneity, and method of incorporation), the mechanical properties depend on the matrix alloy [3].

Clauer and Hansen [4] observed that the formation of a dislocation substructure with dense tangles surrounding Al_2O_3 dispersoids in a pure Al matrix increases the threshold stress and modified the matrix creep properties. Arzt [5] reviewed models for the threshold stress in aluminum containing small volume fractions of submicron dispersoids: climb bypass and detachment mechanisms. Dunand and Jansen [6, 7] considered the effect of dislocation pile-ups upon the detachment threshold stress and presented a model to describe the dislocation creep mechanism for materials with high dispersoid volume fractions.

Some Al-based alloys have been selected as matrix materials due to the additional strengthening behavior from precipitates, in addition to the reinforcements. Oxide reinforced Al-Mg-Si (alloy 6061) has been studied by several researchers [8-13]. Li and Langdon [9] crept 6061-Al reinforced with

irregularly shaped Al_2O_3 particulates and suggested that creep is controlled by viscous glide of dislocations in the matrix. In oxide reinforced Al-Zn (alloy 7005), it was found that creep is controlled by self diffusion of Al [14].

Al-Sc alloys have outstanding mechanical properties due to the presence of elastically hard and coherent Al_3Sc precipitates. These $L1_2$ structured precipitates have a high number density, low coarsening rate, and are stable at elevated temperatures [15-17]. The precipitates have been shown to increase the creep resistance of Al alloys [18-20]. Harada and Dunand [21] reported the activation energy for creep controlled by dislocation climb. Novotny and Ardell [17] investigated the growth kinetics and morphology of the precipitates. Marquis and Seidman [22] confirmed that the coarsening kinetics obey roughly the (aging time)$^{1/3}$ law for average precipitate radius, given by Lifshitz-Slyozov-Wagner (LSW) theory.

This article reports on the microhardness, compressive strength, and creep resistance of an Al-Sc alloy reinforced both with submicron alumina dispersoids and with nanometer-size Al_3Sc precipitates. These mechanical properties are compared to Al-Sc alloys without Al_2O_3 dispersoids and to an Al-Al_2O_3 composite in the absence of Al_3Sc precipitates.

Experimental Material and Procedures

Materials Preparation and Heat-Treatments

A cast alloy Al-0.18 wt.% Sc (referred to as Al-Sc in the following) was prepared from 99.9% Al and an Al-0.5 wt.% Sc master alloy. This material was melted in an alumina crucible, stirred, and then poured into a boron nitride-coated graphite mold. The typical grain diameter of the resulting alloy is 1-2 mm. Average alloy compositions were determined by chemical mass emission analysis (Luvak Inc., Boylston, MA).

Chesapeake Composites Corp. (New Castle, DE) supplied two dispersion-strengthened-cast (DSC) billets. One of the billets, referred to as DSC-Al, was fabricated from 99.98% Al. The second billet, referred to as DSC-Al-Sc, was fabricated from the Al-Sc cast alloy. Both were reinforced with 29.7 to 30.7 vol.% Al_2O_3 dispersoids with a 0.3 μm average diameter. The volume fraction of Al_2O_3 in the tested materials was derived from mass density measurements, via Archimedes method.

Test specimens were machined from the cast billets. Hardness specimens were larger than 5×5×3 mm^3. Cylindrical compression and creep specimens (8.10 mm diameter and 16.10 mm length) were electro-discharge-machined with their axes in the main billet direction. The size of each specimen was measured before and after each test.

As-cast DSC-Al specimens were used in all tests. Aging treatments for Al-Sc and DSC-Al-Sc consisted of homogenization at 640°C in air, water-quenching to room temperature, aging in air at 300 to 450°C, terminated by a room temperature water-quench.

Mechanical Properties

Vickers microhardness measurements were performed on the alloys Al-Sc and DSC-Al-Sc aged at 300 and 350°C for different times. Errors reported are for one standard deviation from the mean value.

Compressive tests at ambient temperature were conducted for DSC-Al-Sc specimens aged at 350°C for 24 h and at 450°C for 60 h. A constant rate of crosshead displacement of 1.0 mm/min was used during testing and the load versus strain curves were recorded continuously by a computer.

Compressive creep experiments at constant load were performed at 300 and 350°C for DSC-Al and DSC-Al-Sc in air in a three-zone resistively heated furnace with a temperature stability of ±1°C. A superalloy compression-cage was used with boron-nitride-lubricated alumina platens. The platen displacement was transmitted by an extensometer connected to a linear voltage displacement transducer (1.0 μm resolution). Strain and loading time were continuously monitored and recorded by computer. At any given stress level, sufficient creep time was allowed to establish a minimum creep rate by weighted linear regression. If the sample had not failed, the load was increased. Therefore, a single specimen could be utilized to obtain the minimum creep rates at different stress levels. Steady-state creep rate was determined after approximately 2% strain, over approximately the last 0.5% strain range. Different aging treatments were utilized for the DSC-Al-Sc specimens, in order to study the effects of distribution and size of Al_3Sc precipitates. Some specimens were used again in creep tests after different aging treatments.

Experimental Results and Discussion

Microhardness

Microhardness curves for Al-Sc and DSC-Al-Sc aged at 300 and 350°C for various times are shown in Figure 1. The four expected regions of precipitation strengthened alloys can be observed in Al-Sc: (a) a short incubation; (b) a rapid increase in microhardness (under-aging); (c) a plateau in microhardness values (peak-aging); and (d) decreasing microhardness (over-aging). Peak-aging occurs at 2 h at 300°C and at 0.5 h for 350°C. Over-aging is more rapid when aged at 350°C. The over-aged hardness appears stable when aged for more than 16 h at 300°C or 6 h at 350°C. The peak hardness for aging at 350°C is lower than that at 300°C by ~19%, while the over-aged hardness as aged at 350°C is lower than that at 300°C by ~8%.

DSC-Al-Sc achieves peak-aging at 4 h at 300°C and at 1 h at 350°C. The hardness decreases after achieving its peak value and then remains almost constant for over 24 h at either 300°C or 350°C. The peak hardness for aging at 350°C is the same as at 300°C within experimental error, while the stable hardness for aging at 350°C is lower than that at 300°C by ~14%. The DSC-Al-Sc peak hardness is ~2.8 times that of Al-Sc when aged at 350°C and ~2.2 times higher when aged at 300°C. This illustrates the hardening from the Al_2O_3 dispersoids, which is independent of aging time or temperature.

A notable difference between the DSC-Al-Sc and Al-Sc curves is that the peak hardness occurs at different times. This suggests that the Al_2O_3 influences the precipitation kinetics of Al_3Sc. A second difference is that peak-aging occurs more rapidly in Al-Sc. This is not in agreement with several previous studies, which suggest that ceramic reinforcements accelerate precipitation due to a higher dislocation density enhancing nucleation and growth [3, 8, 23, 24]. Several previous studies have shown that for some matrix materials at some aging temperatures, aging is decreased or unaffected by the dispersoids [3]. Further investigation is needed to learn why Al_2O_3 decreases the kinetics of Al_3Sc precipitation.

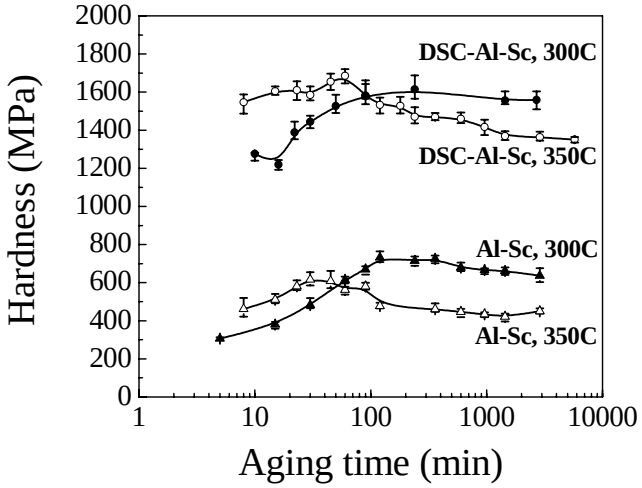

Figure 1: Vickers microhardness (MPa) versus aging time at 300 and 350°C for Al-Sc and DSC-Al-Sc.

Compressive Properties at Ambient Temperature

The compressive stress-strain curves of the DSC-Al-Sc specimens aged at 350°C for 24 h and at 450°C for 60 h are shown in Figure 2. The 0.2% yield strength ($\sigma_{0.2}$), ultimate compressive strength (σ_u) and maximum strain (ε_{max}) corresponding to σ_u are listed in Table I. It is clear that over-aging process causes a lower strength level and deformation capacity since the precipitates coarsened severely during aging at high temperature and long times.

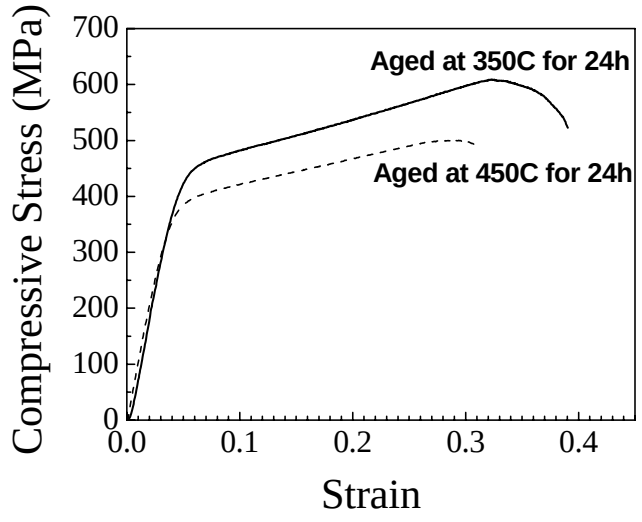

Figure 2: Engineering stress-strain curves for DSC-Al-Sc in compression.

Table I: Compressive Properties of DSC-Al-Sc

Aging Treatment	$\sigma_{0.2}$ (MPa)	σ_u (MPa)	ε_{max}
350°C for 24 h	355	609	0.33
450°C for 60 h	275	500	0.30

Creep Behavior

Figure 3a displays the steady-state creep behavior of DSC-Al and DSC-Al-Sc after different aging treatments, plotted as the minimum creep rate, $\dot{\varepsilon}$, versus applied stress, σ, on double logarithmic axes. It is seen that DSC-Al-Sc has greater creep resistance than DSC-Al. Over-aging leads to an increased creep rate, as seen in Figure 3b. This creep rate is still an improvement over that of DSC-Al.

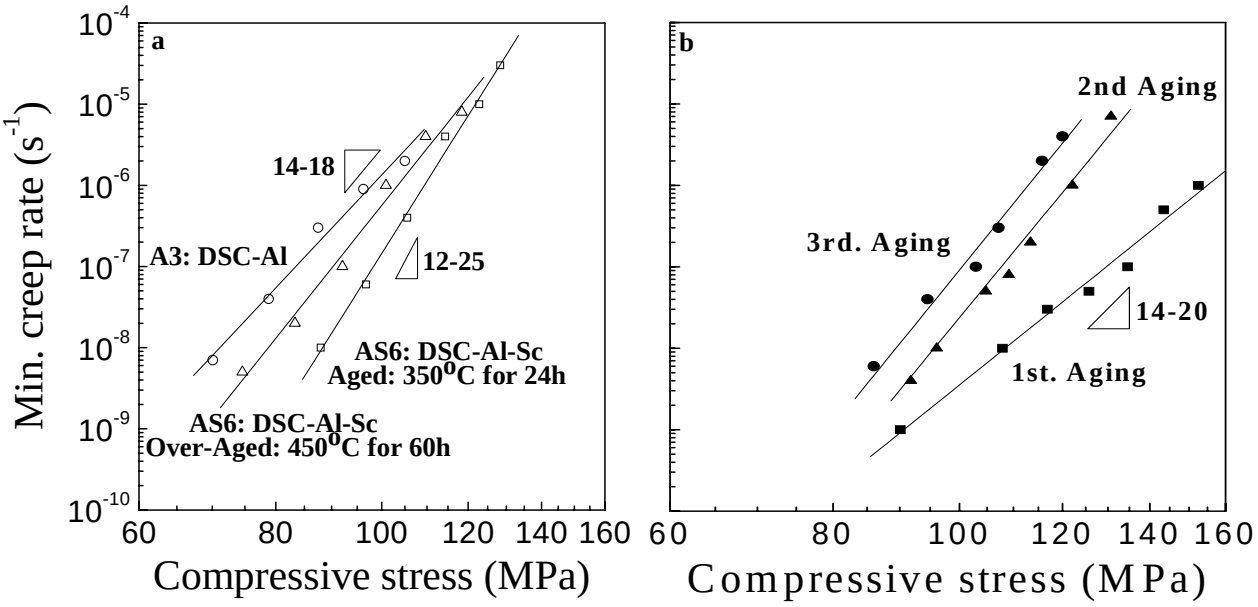

Figure 3: Double logarithmic plots of minimum creep rate versus applied compressive stress. In (a), tested at 350°C, it is seen that DSC-Al-Sc has a lower creep rate and higher apparent stress exponents than DSC-Al. In (b), tested at 300°C, the deleterious impact of over-aging on creep rate is clear. The sample in (b) is AS1, which was aged at 300°C for 24 h, crept, aged at 400°C for 24 h, crept, and aged again at 400°C for 24 h.

The steady-state creep rate of dispersion-strengthened alloys can be described by a power-law equation:

$$\dot{\varepsilon} = A_{ap}\sigma^{n_{ap}} \exp\left(-\frac{Q_{ap}}{RT}\right) \tag{1}$$

where A_{ap} is a dimensionless constant, n_{ap} the apparent stress exponent, Q_{ap} the apparent activation energy, R the ideal gas constant, and T the absolute temperature. Table 2 lists apparent stress exponents for the tested samples. The value of n_{ap} for DSC-Al-Sc is higher than that of DSC-Al. As with other composites and Al-Sc alloys containing no dispersoids, the apparent stress exponents of 12 to 25, are quite high compared with 4.4 for creep controlled by self-diffusion of aluminum [25, 26].

This behavior is justified by accounting for a threshold stress, σ_{th}, below which creep rates are not experimentally measurable. Equation (1) is accordingly modified to yield:

$$\dot{\varepsilon} = A\left(\sigma - \sigma_{th}\right)^{n} \exp\left(-\frac{Q}{RT}\right) \tag{2}$$

where A is a dimensionless constant, n and Q the stress exponent and activation energy of the matrix.

Table II: Creep Properties of DSC-Al and DSC-Al-Sc

Creep Temp. (°C)	Material	Label	Aging Treatment	Estimated Radius* (nm)	n_{ap}	N = 4.4	
						σ_{th} (MPa)	R^2
300	DSC-Al	A1	none	0	7.8	40.7	0.997
	DSC-Al-Sc	AS1	300°C/24 h	2	13.2	80.9	0.930
			as above, crept, 400°C/24 h	10	20.7	87.0	0.901
			as above, crept, 400°C/24 h	19	19.7	79.2	0.934
		AS2	300°C/24 h	2	13.0	78.6	0.969
			as above, crept, 400°C/2 h	6	25.1	106.0	0.945
			as above, crept, 450°C/24 h	30	22.4	94.4	0.978
		AS3	350°C/24 h	4	13.1	78.9	0.903
350	DSC-Al	A3	none	0	14.4	57.2	0.994
		A4	none	0	17.7	65.8	0.964
	DSC-Al-Sc	AS4	350°C/24 h	4	22.7	83.6	0.965
		AS5	450°C/60 h		16.9	69.0	0.969
		AS6	350°C/24 h	4	13.6	67.8	0.972
			as above, crept,450°C/60 h	40	21.5	72.6	0.930
		AS7	350°C/24 h	4	20.3	88.8	0.918
		AS9	400°C/120 h	12	15.1	66.1	0.901
		AS10	450°C/24 h	25	23.3	71.7	0.989
		AS11	350°C/24 h	4	17.9	84.9	0.983

*Radius is estimated from TEM observations of Al-Sc samples with a similar aging treatment [22].

Deformation Mechanism and Threshold Stress. Values for σ_{th} can be found by dividing the intercept by the slope employing a weighted least-squares linear regression of $\sqrt[n]{\dot{\varepsilon}}$ versus σ [27]. The matrix stress exponent n must be selected *a priori*. The choice is made based on the deformation process. It is expected that dislocation motion is the primary deformation mechanism for DSC-Al-Sc. This is appropriate based on the large grain size of the matrix alloy [26]. There are three possible values for the matrix stress exponent: $n = 3$ for viscous glide [28, 29], $n = 5$ for dislocation climb controlled by lattice self diffusion [29-31], and $n = 8$ for constant-structure dislocation climb [32, 33]. We use here the experimentally determined exponent for pure aluminum, $n = 4.4$ [25, 26], which is between the theoretical values for glide and climb, and which has been used in studies on DSC-Al with no Sc [7] and on Al-Sc alloys with no Al_2O_3 [19, 20].

Threshold stresses obtained by linear extrapolation are presented in Table II. Good linear fits are obtained for all samples. The threshold stresses found for Sc-free DSC-Al are in agreement with those in the literature [7]. DSC-Al-Sc has significantly higher threshold stresses than either DSC-Al or literature data for Al-Sc alloys [18-20]. This indicates that strengthening occurs at both length scales, due to the nanometer-sized Al_3Sc precipitates and the sub-micrometer Al_2O_3 particles. A nonlinear effect is also

observed, as DSC-Al-Sc has a higher threshold stress than the sum of stresses of DSC-Al and Al-Sc alloys.

The threshold stress of DSC-Al-Sc increases with aging time because the size of Al_3Sc precipitates increases, as observed and modeled in Al-Sc alloys [18-20]. The radii of precipitates were estimated based on coarsening kinetics in Al-Sc alloys [22]. Because the Al_2O_3 dispersoids are anticipated to change the precipitation kinetics of Al_3Sc, future microanalysis is needed to characterize accurately the size of precipitates. The estimated radii are listed in Table II, and are plotted in Figure 4 against the threshold stress due to the Al_3Sc precipitates (i.e., the threshold stress of DSC-Al is subtracted from all DSC-Al-Sc values). It is seen that the threshold stresses due to Al_3Sc in DSC-Sc-Al are still significantly higher than those of Al-Sc alloys [19, 20], again illustrating the non-linear strengthening effect achieved by a bimodal distribution of unshearable obstacles in aluminum.

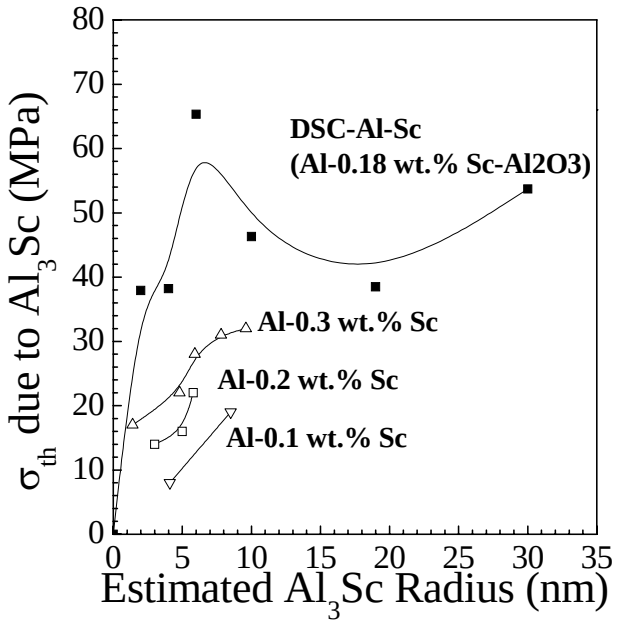

Figure 4: Threshold stress at 300 °C due to Al_3Sc precipitates in DSC-Al-Sc (experimental threshold stress minus DSC-Al threshold stress) as a function of estimated Al_3Sc radius (from data in Ref. [22]). Lines are added to help the eye. The nonlinear additive effect of Al_3Sc precipitates and Al_2O_3 dispersoids is revealed by the fact that the threshold stress due to Al_3Sc is higher in the DSC-Al-Sc materials than in the Al_2O_3-free Al-Sc alloys [19, 20].

Conclusions

A study of DSC-Al-Sc, consisting of an Al matrix with <1 vol.% nanosize Al_3Sc precipitates and 30 vol.% submicron Al_2O_3 dispersoids, yields the following conclusions:

- DSC-Al-Sc exhibits strengthening at ambient temperature from both the Al_3Sc precipitates and the Al_2O_3 dispersoids, as measured by microhardness.

- DSC-Al-Sc tested under compressive creep conditions at 300 and 350 °C exhibits high stress exponents, which are characteristics of materials with a threshold stresses (as also exhibited by DSC-Al or Al-Sc alloys).
- A nonlinear strengthening effect is observed from both populations of particles: DSC-Al-Sc has a threshold stress greater than the sum of the threshold stresses for Al_3Sc-free DSC-Al and Al_2O_3-free Al-Sc alloys.

Acknowledgements

This study was supported by the US Department of Energy through grant DE-FG02-98ER45721. The authors would like to thank Dr. H. Choe (Northwestern University), Dr. C. B. Fuller (Rockwell Scientific), and Dr. E. A. Marquis (Sandia National Laboratories) for useful conversations. Dr. Marquis also prepared the cast Al-Sc alloy. Chesapeake Composites Corp. prepared the DSC-Al and DSC-Al-Sc alloys. We would also like to thank ALCOA for supplying the high purity Al and Ashurst Inc. for supplying the Al-Sc master alloy used in fabricating the alloys. RAK was partially supported by a Walter P. Murphy Fellowship (Northwestern University).

References

1. K. Milicka, J. Cadek, and P. Rys, "Creep of Aluminum Strengthened by Alumina Particles," *Acta Metall*, 18 (7) (1970), 733-746.

2. A. Kelly, "Composites in Context," *Compos Sci Technol*, 23 (3) (1985), 171-199.

3. D.J. Lloyd, "Particle-Reinforced Aluminum and Magnesium Matrix Composites," *Int Mater Rev*, 39 (1) (1994), 1-23.

4. A.H. Clauer, and N. Hansen, "High-Temperature Strength of Oxide Dispersion Strengthened Aluminum," *Acta Metall*, 32 (2) (1984), 269-278.

5. E. Arzt, "Creep of Dispersion Strengthened Materials - a Critical-Assessment," *Res Mech*, 31 (4) (1990), 399-453.

6. D.C. Dunand, and A.M. Jansen, "Creep of Metals Containing High Volume Fractions of Unshearable Dispersoids 1: Modeling the Effect of Dislocation Pile-Ups Upon the Detachment Threshold Stress," *Acta Mater*, 45 (11) (1997), 4569-4581.

7. A.M. Jansen, and D.C. Dunand, "Creep of Metals Containing High Volume Fractions of Unshearable Dispersoids 2: Experiments in the Al-Al_2O_3 System and Comparison to Models," *Acta Mater*, 45 (11) (1997), 4583-4592.

8. J.P. Unsworth, and S. Bandyopadhyay, "Effect of Thermal Aging on Hardness, Tensile and Impact Properties of an Alumina Microsphere-Reinforced Aluminum Metal-Matrix Composite," *J Mater Sci*, 29 (17) (1994), 4645-4650.

9. Y. Li, and T.G. Langdon, “Creep Behavior of an Al-6061 Metal Matrix Composite Reinforced with Alumina Particulates," *Acta Mater*, 45 (11) (1997), 4797-4806.

10. Y. Ma, and T.G. Langdon, “Creep Behavior of an Al-6061 Metal Matrix Composite Produced by Liquid Metallurgy Processing,” *Mat Sci Eng A*, 230 (1-2) (1997), 183-187.

11. Z. Zhou et al., “MMCs with Controlled Non-Uniform Distribution of Submicrometre Al_2O_3 Particles in 6061 Aluminium Alloy Matrix,” *Mater Sci Tech*, 16 (7-8) (2000), 908-912.

12. P. Ganguly, W.J. Poole, and D.J. Lloyd, “Deformation and Fracture Characteristics of AA6061-Al_2O_3 Particle Reinforced Metal Matrix Composites at Elevated Temperatures,” *Scripta Mater*, 44 (7) (2001), 1099-1105.

13. G. Requena et al., “Creep Behaviour of AA 6061 Alloy and AA 6061 Metal Matrix Composite,” *Mater Sci Tech*, 18 (5) (2002), 515-521.

14. Y. Li, and T.G. Langdon, “Creep Behavior of a Reinforced Al-7005 Alloy: Implications for the Creep Processes in Metal Matrix Composites,” *Acta Mater*, 46 (4) (1998), 1143-1155.

15. N. Blake, and M.A. Hopkins, “Constitution and Age Hardening of Al-Sc Alloys,” *J Mater Sci*, 20 (8) (1985), 2861-2867.

16. R.W. Hyland, “Homogeneous Nucleation Kinetics of Al_3Sc in a Dilute Al-Sc Alloy,” *Metall Trans A*, 23 (7) (1992), 1947-1955.

17. G.M. Novotny, and A.J. Ardell, “Precipitation of Al_3Sc in Binary Al-Sc Alloys,” *Mat Sci Eng A*, 318 (1-2) (2001), 144-154.

18. C.B. Fuller, D.N. Seidman, and D.C. Dunand, “Creep Properties of Coarse-Grained Al(Sc) Alloys at 300 Degrees C,” *Scripta Mater*, 40 (6) (1999), 691-696.

19. E.A. Marquis, D.N. Seidman, and D.C. Dunand, “Precipitation Strengthening at Ambient and Elevated Temperatures of Heat-Treatable Al(Sc) Alloys,” *Acta Mater*, 50 (16) (2002), 4021-4035.

20. E.A. Marquis, D.N. Seidman, and D.C. Dunand, “Precipitation Strengthening at Ambient and Elevated Temperatures of Heat-Treatable Al(Sc) Alloys 50(16)(2002), 4021-4035,” *Acta Mater*, 51 (1) (2003), 285-287.

21. Y. Harada, and D.C. Dunand, “Creep Properties of Al_3Sc and Al-3(Sc, X) Intermetallics,” *Acta Mater*, 48 (13) (2000), 3477-3487.

22. E.A. Marquis, and D.N. Seidman, “Nanoscale Structural Evolution of Al3sc Precipitates in Al(Sc) Alloys,” *Acta Mater*, 49 (11) (2001), 1909-1919.

23. S. Arakawa et al., “Effect of Heterogeneous Precipitation on Age-Hardening of Al_2O_3 Particle Dispersion Al-4mass%Cu Composite Produced by Mechanical Alloying,” *Scripta Mater*, 42 (8) (2000), 755-760.

24. J.M. Gomez de Salazar, and M.I. Barrena, "Role of Al_2O_3 Particulate Reinforcements on Precipitation in 7005 Al-Matrix Composites," *Scripta Mater*, 44 (10) (2001), 2489-2495.

25. J.E. Bird, A.K. Mukherjee, and J.E. Dorn, "Correlations between High-Temperature Creep Behavior and Structure" (Paper presented at Quantitative Relation Between Properties and Microstructure, Haifa, Israel,1969), 255-341.

26. H.J. Frost, and M.F. Ashby, *Deformation-Mechanism Maps : The Plasticity and Creep of Metals and Ceramics* (Oxford: Pergamon Press, 1982), 21.

27. R. Lagneborg, and B. Bergman, "The Stress/Creep Rate Behaviour of Precipitation-Hardened Alloys," *Metal Science*, 10 (1) (1976), 20-28.

28. J. Weertman, "Steady-State Creep of Crystals," *J Appl Phys*, 28 (10) (1957), 1185-1189.

29. F.A. Mohamed, and T.G. Langdon, "Transition from Dislocation Climb to Viscous Glide in Creep of Solid-Solution Alloys," *Acta Metall*, 22 (6) (1974), 779-788.

30. J. Weertman, "Steady-State Creep through Dislocation Climb," *J Appl Phys*, 28 (3) (1957), 362-364.

31. F.A. Mohamed, and T.G. Langdon, "The Transition from Dislocation Climb to Viscous Glide in Creep of Solid Solution Alloys," *Acta Metall*, 22 (6) (1974), 779-788.

32. O.D. Sherby, R.H. Klundt, and A.K. Miller, "Flow-Stress, Subgrain Size, and Subgrain Stability at Elevated-Temperature," *Metall Trans A*, 8 (6) (1977), 843-850.

33. G. Gonzalez-Doncel, and O.D. Sherby, "High Temperature Creep-Behavior of Metal Matrix Aluminum-SiC Composites," *Acta Metall Mater*, 41 (10) (1993), 2797-2805.